

Anisotropic surface impedance of $\text{YBa}_2\text{Cu}_3\text{O}_{7-\delta}$ single crystals

Jian Mao, D. H. Wu, J. L. Peng, R. L. Greene, and Steven M. Anlage

Center for Superconductivity Research, Physics Department, University of Maryland, College Park, Maryland 20742

(Received 28 September 1994; revised manuscript received 15 November 1994)

The anisotropic surface resistance R_{s-ab} and R_{s-c} as well as the penetration depth λ_{ab} and λ_c of $\text{YBa}_2\text{Cu}_3\text{O}_{7-\delta}$ single crystals have been measured at 9.6 GHz. $\lambda_c(T)$ and $\lambda_{ab}(T)$ are linear in temperature at low temperatures with much different slopes, consistent with the existence of line nodes on a cylindrical Fermi surface. A collapse of the c -axis scattering rate below T_c is also observed, and the temperature dependence of the ab plane scattering rate is consistent with quasiparticle-quasiparticle scattering. The behavior of $\lambda_c(T)$ is not consistent with proximity-effect models, or with cubic $d_{x^2+y^2-z^2}$ pairing symmetry, but is consistent with a cubic $d_{x^2-y^2}$ pairing state.

The symmetry of the ground-state wave function is one of the most important problems in the study of cuprate superconductors today. Some models postulate that the pairing mechanism involves the exchange of antiferromagnetic spin fluctuations.¹ Monte Carlo calculations based on the Hubbard model suggest that pairing occurs in the $d_{x^2-y^2}$ channel.² The gap function for this state has the form $\Delta(k) = \Delta_0[\cos(k_x a) - \cos(k_y b)]$, and exhibits line nodes parallel to the c direction on a cylindrical Fermi surface. The result, in the absence of impurity broadening, is a density of states that increases as $E - E_F$ with respect to the Fermi energy at low energy. This linear energy dependence implies that all components of the magnetic penetration depth $\lambda(T)$ should exhibit a linear temperature dependence at low temperatures.³⁻⁵

Recently, a number of experimental results and theoretical interpretation of the results suggest two-dimensional (2D) d -wave superconductivity in the ab plane of hole-doped cuprate superconductors such as $\text{YBa}_2\text{Cu}_3\text{O}_{7-\delta}$ (YBCO).⁶⁻⁹ However, other theoretical models have been proposed to explain the linear temperature dependence of $\lambda_{ab}(T)$. Klemm explained the $\lambda_{ab}(T)$ data of Hardy *et al.*⁸ in YBCO quantitatively, based upon proximity coupling between one s wave superconducting and one normal layer per unit cell.¹⁰ He also suggested measurements of $\lambda_c(T)$ as a way to conclusively distinguish the pairing state symmetry. Another theory proposed by Chakravarty *et al.*¹¹ features low T_c pairing in each copper oxide layer enhanced by Josephson pair tunneling between layers. There is an experiment suggesting that the electrodynamic properties in the superconducting state along the c axis of $\text{La}_{2-x}\text{Sr}_x\text{CuO}_4$ can be explained by a similar Josephson-coupled layer model,¹² although no conclusion was made about the pairing state symmetry.

In principle, one should be able to use c -axis surface impedance measurements to measure the anisotropy of the gap and put further constraints on the pairing state symmetry.^{3,4} The properties of the superconducting state in the c direction of YBCO, such as the penetration depth, surface resistance R_s , and conductivity σ , are still not clear. In this paper we measure $\lambda_c(T)$, R_{s-c} , and σ_c of YBCO single crystals to shed further light on the pairing state symmetry of the cuprates.

YBCO single crystals are grown in zirconia crucibles by

the standard flux method.¹³ We chose samples with minimum twinning and smooth shiny surfaces with typical crystal sizes of about $1 \text{ mm} \times 1 \text{ mm} \times 15\text{--}25 \text{ }\mu\text{m}$. Rutherford back scattering channeling yield is $\leq 4\%$ at room temperature, indicative of high quality. The crystals typically show zero resistance at 92–93 K in dc resistivity measurements. ac and dc magnetization measurements also confirm the transition temperature to be 92–93 K with the transition width less than 0.25 K. The normal-state resistivity at 100 K is about 40–50 $\mu\Omega \text{ cm}$ by dc measurement, similar to that of the Illinois crystals¹⁴ and substantially less than $\sim 70 \text{ }\mu\Omega \text{ cm}$ of the University of British Columbia group.⁶

The surface impedance measurements were made by a cavity perturbation method.¹³ The cylindrical Nb cavity was thermally treated in an ultra high vacuum to recrystallize the surfaces, and was kept submerged in liquid helium at 4.2 K during the experiments. The surface resistance and the penetration depth data are obtained via the simultaneous measurement of the quality factor Q and the resonant frequency f_0 of the cavity as a function of the sample temperature. The surface impedance is obtained from the Q and f_0 using

$$R_s = \Gamma(1/Q - 1/Q_{\text{cav}}), \quad \Delta X_s = 2\pi f_0 \mu_0 \Delta \lambda, \quad (1)$$

$$\Delta \lambda = -\zeta(\Delta f_0 - \Delta f_{0-\text{cav}}),$$

where Q_{cav} ($\sim 2.3 \times 10^7$ at 4.2 K and 9.6 GHz) and $\Delta f_{0-\text{cav}}$ are the quality factor and frequency shift of the cavity without sample, respectively. Γ and $\zeta = \Gamma/\pi\mu_0 f_0^2$ are the geometric factors which depend on the resonant mode, the size of the cavity, and the sample size and shape. With the high Q , we have a resolution of $\Delta(1/Q) \sim 5 \times 10^{-10}$ and $\Delta f_0 \sim 1 \text{ Hz}$ translating to $\Delta R_s \leq 50 \text{ }\mu\Omega$ and $\Delta \lambda \leq 3 \text{ \AA}$ for a typical YBCO crystal. Note that in contrast to lower frequency measurements,⁸ we do not need to consider a finite thickness correction because in our frequency range the ab plane and c -axis skin depths are far less than the corresponding sample dimensions.¹⁵

To study the anisotropy of YBCO, we measure the crystals in two orientations: in experiment I, the c axis of the crystal is parallel to the rf magnetic field; in experiment II, the c axis is perpendicular to the rf magnetic field (see the inset of Fig. 1). Assume the crystal has width l , height h , and

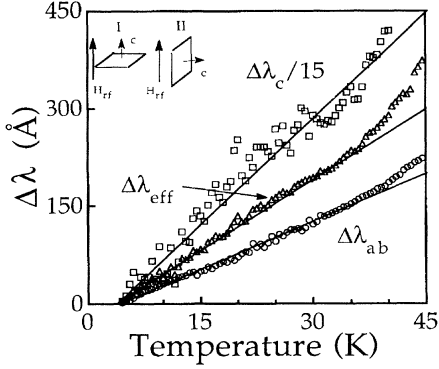


FIG. 1. Temperature dependence of the penetration depth $\Delta\lambda = \lambda(T) - \lambda(4.2 \text{ K})$ in a YBCO single crystal. Solid lines are the linear fits. The inset shows the orientation of the crystal in the two experiments.

thickness t . In experiment I, the rf current runs in the ab plane, and the complex loss is $K_{s-ab}^2 t(l+h)MZ_{s-ab}$, where K_{s-ab} is the induced surface supercurrent, $Z_s = R_s + iX_s$, and M is the demagnetization factor. As the supercurrent flows only in the ab plane, we measure just λ_{ab} and R_{s-ab} . In this configuration, because the rf field is perpendicular to the large sample surface area, the demagnetization factor becomes large and makes the calculation of the geometrical factors Γ and ζ of Eq. (1) difficult.^{13,15} Therefore Γ and ζ were determined by comparing the normal-state surface resistance at 100 K with the dc resistivity $\rho_{ab}(100 \text{ K}) \approx 40 \mu\Omega \text{ cm}$. As a check, a Nb crystal of known resistivity and similar size was used to independently determine the geometric factors.¹³ In this case we found $R_s(T > T_c) \approx X_s(T > T_c)$ for both the YBCO and Nb crystals.

In experiment II, the demagnetization factor is approximately one. The geometric factors Γ and ζ in Eq. (1) can be calculated precisely and are in excellent agreement with the experimental data on the Nb crystal placed in this orientation.¹⁶ The complex loss is given by $K_{s-eff}^2 h(l+t)Z_{s-eff} = K_{s-eff}^2 h t Z_{s-c} + K_{s-eff}^2 h l Z_{s-ab}$, where K_{s-eff} is the induced surface supercurrent flowing along the a - (or b -) and c -axis directions, and $Z_{s-eff} = R_{s-eff} + i\mu_0\omega\lambda_{eff}$. The c -axis penetration depth λ_c , and surface resistance R_{s-c} can be extracted from experiments I and II as

$$\begin{aligned} \lambda_c &= [\lambda_{eff}(l+h) - \lambda_{ab}l]/t, \\ R_{s-c} &= [R_{s-eff}(l+h) - R_{s-ab}l]/t. \end{aligned} \quad (2)$$

The extraction of λ_c and R_{s-c} has been done for several crystals of different thickness t , and the results are qualitatively similar. In this paper, we will analyze the properties of one crystal in detail and point out the degree to which its properties reflect those of all the samples.

Figure 1 shows $\Delta\lambda = \lambda(T) - \lambda(4.2 \text{ K})$ for $\Delta\lambda_{ab}$, $\Delta\lambda_{eff}$ and $\Delta\lambda_c/15$ for a YBCO crystal. The strong linear temperature dependence extends up to 40 K in λ_{ab} and λ_{eff} , and therefore λ_c . The slope $d\lambda_{ab}/dT = 5 \text{ \AA/K}$, slightly bigger than 4.3 \AA/K reported by the UBC group,⁸ is consistent with the clean d -wave model for a superconductor with line nodes in the gap.^{4,17} As for the penetration depth along the c axis, the slope is $d\lambda_c/dT \approx 130 \pm 15 \text{ \AA/K}$ (we find that the exact

values of these slopes vary from sample to sample). Recently, Klemm and Liu calculated $\lambda_c(T)$ using a multilayer proximity model, and their $\lambda_c(T)$ shows an activated behavior at low temperatures.¹⁰ Our result that $\Delta\lambda_c(T)$ is linear at low temperatures is consistent with the d -wave model and not with the multilayer proximity model. Also, an extrinsic proximity effect model which supposes that a normal-metal dead layer exists on the surface of the YBCO crystal,¹⁸ cannot account for either the ab plane or c -axis penetration depth measured here.¹⁹

To determine the absolute magnitude of the penetration depth in experiment I, we assume YBCO is in the London limit [$\lambda \gg \xi(0)$] and use the identity $X_s(4.2 \text{ K})/R_s(100 \text{ K}) = 2\lambda(4.2 \text{ K})/\delta$, where δ is the skin depth, to deduce the value of penetration depth at 4.2 K.²⁰ Since $X_s = \mu_0\omega\lambda$, we have $X_s(4.2 \text{ K}) = X_s(100 \text{ K}) - \omega\mu_0\Delta\lambda$, where $\Delta\lambda$ is the measured penetration depth change from 4.2 to 100 K and $X_s(100 \text{ K}) = R_s(100 \text{ K}) = (\omega\mu_0\rho_{dc}/2)^{1/2}$ in the normal skin-effect regime. We obtain $\lambda_{ab}(4.2 \text{ K}) = 1250 \text{ \AA}$, and if we assume the linear behavior continues below 4.2 K, this extrapolates to $\lambda_{ab}(0) = 1230 \text{ \AA}$. An alternative (and somewhat arbitrary) method for estimating $\lambda_{ab}(0)$ is to plot $\Delta\lambda$ vs y , where $y = 1/[1-t^4]^{1/2}$ is the Gorter-Casimir temperature dependence, $t = T/T_c$, and T_c is chosen to be 90.5 K .²¹ When the data is plotted in this way, we obtain a straight line from 75 K up to 90.4 K with a slope giving $\lambda_{ab}(0) = 1200 \text{ \AA}$, nearly equal to the value obtained above. In experiment II, we cannot determine $\lambda_{eff}(0)$ using the normal-state impedance as $X_{s-eff}(T > T_c) \neq R_{s-eff}(T > T_c)$.^{15,16} However, applying the Gorter-Casimir relation in the same way, we obtain an estimated value of $\lambda_{eff}(0) = 1380 \text{ \AA}$. Assuming the linear temperature dependence between 4.2 and 40 K can be extrapolated to 0 K, we have $\lambda_{eff}(4.2 \text{ K}) = 1415 \text{ \AA}$. All the $\lambda(0)$ values determined here are in the range of reported values^{8,22} and they are not strongly dependent on the $\lambda(T)$ extrapolation or T_c value assumed, although they do vary by $\approx 20\%$ from sample to sample. From Eq. (2), we extract $\lambda_c(0) \approx 1.05 \mu\text{m}$. The anisotropy of the magnetic penetration depth, $\lambda_{ab}/\lambda_c \sim 9$ for $T \leq T_c/2$, in good agreement with recent estimates made from infrared reflectivity measurements.²³

Annett *et al.*³ predicted that a superconducting state with four line nodes parallel to the c axis on a cylindrical Fermi surface will show $\Delta\lambda_{ab}(T)/\lambda_{ab}(0) \sim \alpha(T/T_c) + \beta(T/T_c)^3$, and $\Delta\lambda_c(T)/\lambda_c(0) \sim \gamma(T/T_c)$ at low temperatures. We find excellent fits to $\Delta\lambda_{ab}(T)$ of this form up to $T/T_c = 0.65$ with $\alpha = 0.32$, $\beta = 0.29$; however, linear fits to $\lambda_c(T)$ with $\gamma \approx 1.5$ are good only for $T/T_c < 0.3$.

Figure 2 shows the normalized superfluid density $[\lambda(0)/\lambda(T)]^2$, which is also proportional to the imaginary part σ_2 of the complex conductivity $\sigma = \sigma_1 - i\sigma_2$. The superfluid density along the c axis is depleted linearly at low temperatures, but much faster than in the ab plane, with less than 10% remaining for temperatures above 50 K. At temperatures $0.35 < T/T_c < 1$, $[\lambda_c(0)/\lambda_c(T)]^2$ is proportional to $(T - T_c)/T^2$,²⁴ resembling the calculation of $1/\lambda_c(T)^2$ for a $d_{x^2-y^2}$ superconductor with a spherical Fermi surface.⁴ In addition, the calculation of $\sigma_{2c}(T)$ for the cubic $d_{x^2+y^2-z^2}$ state does not resemble our data.

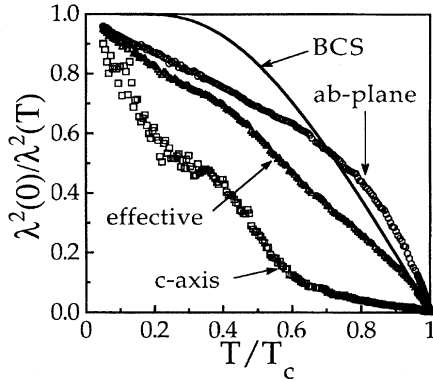


FIG. 2. $\lambda^2(0)/\lambda^2(T)$ vs T/T_c for λ_c , λ_{ab} , and λ_{eff} in a YBCO crystal. Data for λ_{ab} and λ_{eff} are experimental results. Data for λ_c are extracted from λ_{ab} and λ_{eff} . Solid line is the weak-coupled BCS s -wave calculation.

The steep drop of the superfluid density along the c axis and ab plane at low temperatures is in remarkable contrast to that of the BCS s -wave calculation, which is shown by the solid line in Fig. 2. The slopes of $[\lambda(0)/\lambda(T)]^2$ at $T/T_c=1$ for the ab plane is about 4.06, and for the c axis it is about 0.37, whereas the weak-coupled BCS theory gives a value for this slope of exactly 2 in the London limit.²⁵ This value for the slope in the ab plane is larger than any conventional superconductor,²⁵ while the slope for the c direction is comparable to the weak-coupled limit of a cubic d -wave superconductor.²⁶

Figure 3 shows the surface resistance in the ab plane, and the effective surface resistance, which contains the contribution from the c -axis component. The losses drop by three orders of magnitude in a few degrees below T_c , reach a minimum around 70 K, and then increase to a maximum around 40 K for R_{s-ab} and 30 K for R_{s-c} before falling down again. The lowest value of $R_{s-ab} \sim 165 \mu\Omega$ at the minimum dip around 70 K (210 $\mu\Omega$ at 77 K) is among the lowest reported surface resistance values measured at 10 GHz near 77 K.²⁷ The normal state $R_s(T)$ and $X_s(T)$ imply a metallic temperature dependence for $\rho_c(T)$, with a value $\rho_c(100 \text{ K}) \approx 4 \text{ m}\Omega \text{ cm}$, consistent with values obtained by c -axis transport¹⁴ and infrared reflectivity.^{23,28}

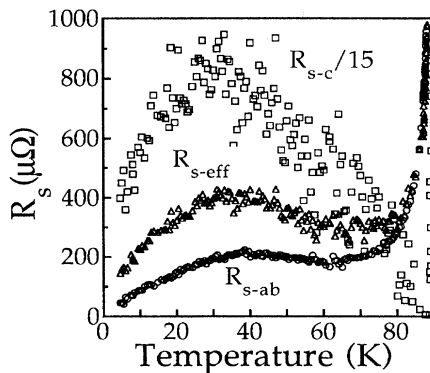


FIG. 3. Surface resistances for $R_{s,ab}$, $R_{s,\text{eff}}$, and $R_{s,c}/15$ of a YBCO crystal. Data for $R_{s,c}$ is extracted from $R_{s,ab}$ and $R_{s,\text{eff}}$.

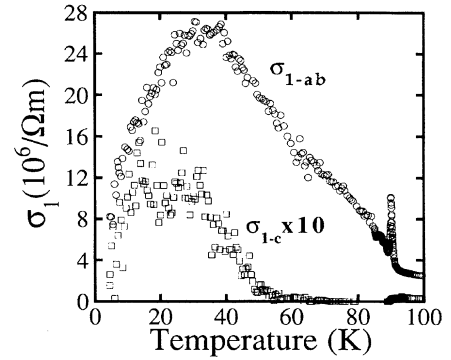


FIG. 4. The real part of conductivity σ_{1-ab} and $10\times\sigma_{1-c}$ as a function of temperature for a YBCO crystal.

Because we measure both R_s and ΔX_s simultaneously, we can determine $\sigma_1(T)$ using the fewest assumptions.^{6,20} Figure 4 shows the real part of the complex conductivity σ_1 along the c direction and in the ab plane. There is no residual resistance subtraction from R_{s-ab} , while for R_{s-c} , about 5 m Ω was subtracted to make $\sigma_{1-c}(T \rightarrow 0) \rightarrow 0$ in Fig. 4. From Fig. 4, we can clearly see that there are two peaks in σ_{1-ab} : a broad peak centered around 30 K and sharp peak near T_c . In σ_{1-c} , the first peak occurs between 15 and 30 K, and the conductivity in the c direction is at least 30 times less than that of the ab plane. In the clean d -wave model, one expects $\sigma_1(T) \sim T^2$ at low temperatures.¹⁷ However, we see a sublinear temperature dependence for $\sigma_1(T)$ in both the ab plane and c -axis directions at low temperatures.

The second sharp peak in $\sigma_{1-ab}(T)$ occurs just below T_c precisely at the point where $\sigma_2 = \sigma_1$, and it is not seen in data on Nb crystals. This peak in σ_1 may be due to inhomogeneities which broaden the transition, and/or enhanced fluctuations in the microwave conductivity near T_c .²¹ The peak in Fig. 4 is among the sharpest ever seen⁶ and if it is due to inhomogeneity, it is a sign that all YBCO crystals studied to date are by no means “ideal.”

A two-fluid interpretation of the c -axis conductivity leads to qualitatively similar conclusions as those obtained for the ab -plane results by the UBC group.^{6,29} We find that both $1/\tau_{ab}(T)$ and $1/\tau_c(T)$ fall dramatically below T_c , although neither clearly follows the $(T/T_c)^3$ form predicted by the d -wave model,^{17,30} with $1/\tau_{ab}(4.2 \text{ K}) \sim 10^{11} \text{ Hz}$ and $1/\tau_c(4.2 \text{ K}) \sim 3 \times 10^{11} \text{ Hz}$.³¹ The ab -plane scattering rate is better described as $1/\tau_{ab}(T) \sim x_{n,ab}(T)^p$ where $p \sim 2.1-2.4$ (for ab -plane normal fluid fraction $x_{n,ab} > 0.25$), and $p < 1/2$ (for $x_{n,ab} < 0.25$), perhaps indicative of quasiparticle-quasiparticle scattering at high temperatures, and residual scattering at lower temperatures. The c -axis scattering rate reaches its residual value below about 10 K, and its value is somewhat smaller than a recent far-infrared determination of 85 cm^{-1} ($\sim 2.6 \times 10^{12} \text{ Hz}$).²³ This low value of the residual scattering rate is consistent with our observation of a “clean-node” $\Delta\lambda_c(T) \sim T$ at low temperatures.^{3,5} It may also mean that nonlocal electrodynamic corrections could become important in YBCO at low temperatures.

Our results for $\sigma_{1c}(T)$ and $\lambda_c(T)$ in YBCO are rather different from other recent measurements of c -axis properties in related cuprate materials. s -wave-like temperature

dependencies have been seen in the c -axis plasma frequency of $\text{YBa}_2\text{Cu}_4\text{O}_8$ by Basov *et al.*,³² and in $\lambda_c(T)$ of $\text{La}_{2-x}\text{Sr}_x\text{CuO}_4$ by Shibauchi *et al.*¹² The samples measured by Basov *et al.* had no coherent Drude-like component in the low frequency conductivity and are thought to be naturally underdoped³² whereas our samples, like those of Schützmann *et al.*,²³ have a metallic c -axis conductivity above T_c . This suggests that the c -axis electrodynamic properties may be very sensitive to doping (since the low resistivities of our samples, and the low T_c of Schützmann's samples suggest that they are overdoped), as well as to the particular layered structure of each cuprate material.

In summary, we have measured the surface impedance of the same high quality YBCO crystal along the c axis and in the ab plane. The low temperature part of $\lambda_c(T)$ and

$\lambda_{ab}(T)$ show linear behavior, which is consistent with line nodes in the c direction on a cylindrical Fermi surface. There is a collapse of the c -axis quasiparticle scattering rate below T_c which closely parallels the ab -plane quasiparticle dynamics. The overall anisotropic surface impedance temperature dependence is not consistent with either intrinsic or extrinsic proximity-effect models, but is surprisingly consistent with a cubic 3D $d_{x^2-y^2}$ pairing state, except for the temperature dependence of $\sigma_1(T)$ at low temperatures.

The authors would like to acknowledge Dr. P. Hirschfeld and Dr. R. P. Huebener for discussions, Dr. R. P. Sharma for RBS results, and the NSF NYI program (Grant No. DMR-9258183), NSF Grant No. DMR-9123198, and NSF Grant No. DMR-9209668 for support.

-
- ¹N. E. Bickers, D. J. Scalapino, and S. R. White, Phys. Rev. Lett. **62**, 961 (1989).
- ²N. Bulut, D. J. Scalapino, and S. R. White, Phys. Rev. B **47**, 14 599 (1993).
- ³J. Annett, N. Goldenfeld, and S. R. Renn, Phys. Rev. B **43**, 2778 (1991).
- ⁴M. Prohammer and J. P. Carbotte, Phys. Rev. B **43**, 5370 (1991).
- ⁵P. J. Hirschfeld and N. Goldenfeld, Phys. Rev. B **48**, 4219 (1993).
- ⁶D. A. Bonn *et al.*, Phys. Rev. B **47**, 11 314 (1993).
- ⁷Z.-X. Shen *et al.*, Phys. Rev. Lett. **70**, 1553 (1993).
- ⁸W. N. Hardy *et al.*, Phys. Rev. Lett. **70**, 3999 (1993).
- ⁹D. A. Wollman *et al.*, Phys. Rev. Lett. **71**, 2134 (1993).
- ¹⁰R. A. Klemm and Samuel H. Liu (unpublished).
- ¹¹S. Chakravarty *et al.*, Science **261**, 337 (1993).
- ¹²T. Shibauchi *et al.*, Phys. Rev. Lett. **72**, 2263 (1994).
- ¹³S. M. Anlage *et al.*, Phys. Rev. B **50**, 523 (1994).
- ¹⁴T. A. Friedmann *et al.*, Phys. Rev. B **42**, 6217 (1990).
- ¹⁵C. E. Gough and N. J. Exon, Phys. Rev. B **50**, 488 (1994).
- ¹⁶For Nb, we found $R_s(T > T_c) \approx X_s(T > T_c)$; but in the case of YBCO, $X_{s\text{-eff}}(T > T_c)$ is always slightly ($\sim 10\%$) bigger than $R_{s\text{-eff}}(T > T_c)$.
- ¹⁷J. L. Hirschfeld, W. O. Putikka, and D. J. Scalapino, Phys. Rev. Lett. **71**, 3705 (1993).
- ¹⁸E. F. Skelton *et al.*, Science **263**, 1416 (1993).
- ¹⁹M. S. Pambianchi, J. Mao, and S. M. Anlage, Phys. Rev. B **50**, 13 659 (1994).
- ²⁰O. Klein, E. J. Nicol, K. Holczer, and G. Gruner (unpublished).
- ²¹Mean field behavior of $\lambda(T)$ is not observed near T_c , hence fits to the Gorter-Casimir model were made outside the critical regime. See S. Kamal *et al.*, Phys. Rev. Lett. **73**, 1845 (1994) and S. M. Anlage *et al.* (unpublished).
- ²²K. Zhang *et al.*, Phys. Rev. Lett. **73**, 2484 (1994).
- ²³J. Schützmann *et al.*, Phys. Rev. Lett. **73**, 174 (1994).
- ²⁴The details of $\sigma_{2c}(T)$ are not reproducible from crystal to crystal, however, the general features that $\sigma_{2c}(T)$ is linear in T at low temperatures and shows upward curvature at higher temperatures are seen in all crystals. The temperature dependence of σ_{2c} is reminiscent of the Josephson-coupling model of Refs. 12 and 32 with an SNS-like $J_c(T)$.
- ²⁵F. Marsiglio, J. P. Carbotte, and J. Blezius, Phys. Rev. B **41**, 6457 (1990).
- ²⁶H. Chi and J. P. Carbotte, Phys. Rev. B **49**, 6143 (1994).
- ²⁷YBCO crystals measured at 34.8 GHz in Ref. 22 extrapolate to $R_{\text{sub}} \sim 140 \mu\Omega$ or $205 \mu\Omega$ (using ω^2 or $\omega^{1.7}$ scaling, respectively) at 10 GHz.
- ²⁸C. C. Homes *et al.*, Phys. Rev. Lett. **71**, 1645 (1993).
- ²⁹Applying the two-fluid model to the c -axis data is problematic because it is not clearly in the clean limit. See D. A. Bonn *et al.*, Phys. Rev. Lett. **72**, 1391 (1994). However, we shall assume that $\xi_c/l_{mfp,c} < 1$ at all temperatures, so that the c -axis electrodynamic is never in the extreme dirty limit.
- ³⁰S. M. Quinlan, D. J. Scalapino, and N. Bulut, Phys. Rev. B **49**, 1470 (1994).
- ³¹In the scattering rate analysis, residual normal fluid fractions x_{n0} of 2% and 31% are added for the ab plane and c axis, respectively, to keep $f(\omega\tau) \leq \frac{1}{2}$ (see Ref. 6). However, if one uses the constraint that $f(\omega\tau)$ approaches its low temperature value with zero slope, one finds x_{n0} of 5% and $\sim 50\%$, respectively.
- ³²D. N. Basov *et al.*, Phys. Rev. B **50**, 3511 (1994).